ACS OMEGA

http://pubs.acs.org/journal/acsodf

Article

Conformation of a Comb-like Chain in Solution: Effect of Backbone Rigidity

Xinghong Mai,[#] Peng Hao,[#] Danfeng Liu, and Mingming Ding*

Cite This: *ACS Omega* 2023, 8, 11177−11183

Read Online

ACCESS | Metrics & More | Article Recommendations

ABSTRACT: We study the effect of backbone rigidity on the conformation of comb-like chains in dilute solution by using Brownian dynamics simulations. Our results demonstrate that the backbone rigidity can control the effect of side chains on the conformation of comb-like chains; that is, the relative strength of the excluded-volume interactions from backbone monomer-graft and graft−graft to backbone monomer−monomer gradually weakens with the increase of backbone rigidity. Only when the rigidity of the backbone tends to be flexible and the grafting density is high is the effect of excluded volume of graft−graft on the conformation of comb-like chains significant enough, and other cases can be ignored. Our results show that the radius of gyration of comb-like chains and the persistence length of the backbone are exponentially related to the stretching factor, where the power exponent exhibits an increase with the increase of the strength of bending energy. These finds provide new insights for characterizing the structure properties of comb-like chains.

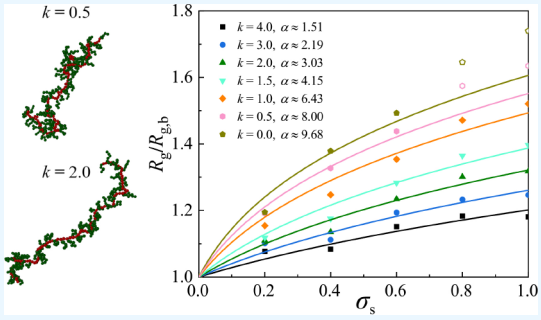

1. INTRODUCTION

Comb-like polymers are branched polymers with a linear backbone grafted by multiple side chains[1−9] that have emerged as an intriguing class of materials for a wide range of potential applications, including supersoft elastomers, nanocarriers, surfactants, and stimuli-responsive coatings.[10−15] Compared with homologous linear polymers, the side chains provide additional steric repulsions, resulting in considerable stiffening of the backbone or even the side chains, which is the origin of many special physical and chemical properties. Three molecular parameters, the degree of polymerization of backbone (N_b), the degree of polymerization of side chains (N_g) and the grafting density (σ_s), which is defined as the reciprocal of the degree of polymerization between two neighboring branching points, constitute a set describing the conformations of comb-like polymers. Therefore, it requires quantitative knowledge between the molecular parameters and the conformations of comb-like polymers to lay a foundation for various applications.

Theoretically, many researchers have proposed a variety of different models to explain the influence of steric repulsions caused by side chains on the conformation of comb-like chains.[16−22] Among them, the Flory approximation is more used due to its simplicity, where the free energy of comb-like polymers is composed of the entropic elasticity and the excluded-volume interactions, i.e.

$$\frac{\Delta F}{k_B T} = \frac{3R_g^2}{2N_b a^2} + \frac{\upsilon_1 a^3 N_b^2}{R_g^3} + \frac{\upsilon_2 V^3 \sigma_s N_b^2}{R_g^3} + \frac{\upsilon_3 R_m^3 \sigma_s^2 N_b^2}{R_g^3} \quad (1)$$

Here, k_B denotes the Boltzmann constant and T represents the absolute temperature, respectively. Because the degree of polymerization of side chains is often much smaller than that of the backbone, the elastic entropy in the first term on the right side of eq 1 only includes the contribution of the backbone, where R_g represents the radius of gyration and a is the Kuhn length. The second, third, and fourth terms represent the excluded-volume interactions, where $\upsilon_1 a^3$, $\upsilon_2 V^3$, and $\upsilon_3 R_m^3$ are the backbone monomer−monomer excluded volume, the backbone monomer−graft excluded volume, and the graft−graft excluded volume, respectively. Minimizing with respect to R_g, we can get

$$\frac{R_g}{R_{g,b}} = \left(1 + \frac{\upsilon_2 V^3}{\upsilon_1 a^3}\sigma_s + \frac{\upsilon_3 R_m^3}{\upsilon_1 a^3}\sigma_s^2\right)^{1/5} \quad (2)$$

where $R_{g,b}$ is the radius of gyration of backbone. Simplified further, it can be written as

Received: December 17, 2022
Accepted: March 9, 2023
Published: March 17, 2023

$$R_g/R_{g,b} = (1 + \alpha\sigma_s + \beta\sigma_s^2)^{1/5} \quad (3)$$

where α and β denote two prefactors that reflect the relative strength of the excluded-volume interactions from backbone monomer−graft and graft−graft to backbone monomer−monomer, respectively.

Recent advances in polymerization techniques have made possible the synthesis of comb-like chains with well-controlled molecular architectures, yielding characterizing data for their structure properties in experiments. For example, by grafting short poly(ethylene glycol) (PEG) onto methylcellulose (MC), Lodge et al. demonstrated that the effect of a graft−graft excluded-volume interaction on the dimensions of comb-like chains can be ignored ($\beta = 0$ in eq 3) when the grafting density is in the range of $0.07 < \sigma_s < 0.33$.[21,23] Conversely, via a set of poly(propargyl acrylate) (PPA)-*g*-polystyrene (PS) comb-like samples, Li et al. found that the effect of the graft−graft excluded-volume interaction always exists at different grafting densities.[24−26] With the advantage of accurate and controllable molecular parameters, numerous simulation works have explored the relationship between the microscopic conformational details and the molecular parameters from the molecular level.[27−34] Recently, using Brownian dynamics (BD) simulations, we found that the dimensions of comb-like chains and the stretching factor ($\sigma_s N_g$) satisfy a quantitative exponential relationship, which qualitatively validates the different experimental results.[35]

Although the academic community has made significant progress in theory, experiment, and simulation, the effect of backbone rigidity on the conformation of comb-like chains has not been paid attention, which may be one of the core factors that make it difficult to compare different results. For example, in experiments, the selection of backbone is not arbitrary but depends on the selected synthesis methods, such as MC and PPA mentioned above, which are different in their own softness.[21,23−26] For theoretical and simulation works, more attention is paid to the impact of the introduction of side chains on the stiffness of the backbone. For example, Hsu et al. reported a series of works explaining the impact of the side chains in bottle-brush chains on the persistence length of the backbone and the entire conformation and compared with the experimental results.[36−39] However, the existing studies do not distinguish the "intrinsic" rigidity (persistent length) of the backbone and the "induced" rigidity due to the steric repulsions resulting from the side chains. Therefore, clarifying the effect of backbone rigidity on the excluded-volume interactions of backbone monomer−graft and graft−graft can afford new insights for characterizing structure properties of comb-like chains.

In this paper, we study the effect of backbone rigidity on the conformation of comb-like chains by using BD simulations. Our article is structured as follows: In section 2, we focus on the simulation details and specific parameters. In section 3, we discuss the effect of backbone rigidity on the conformation of comb-like chains and find the relative strength of the excluded-volume interactions from backbone monomer−graft and graft−graft to backbone monomer−monomer gradually weakens with the increase of backbone rigidity. In section 4, we draw some conclusions and provide an overview.

2. MODEL AND METHODS

As shown in Figure 1a, a coarse-grained model in which a comb-like chain is modeled as a bead−spring chain consisting of N_b backbone beads and N_g beads for one side chain is used in the current study, which is commonly adopted in relevant reports.[3,27,28,30,32,35,38,40−43] We use the purely repulsive Lennard-Jones (LJ) potential to account for the excluded-volume interactions between two beads,[44] i.e.

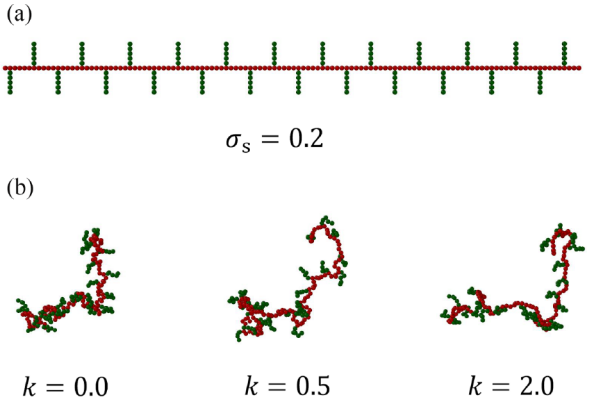

Figure 1. (a) Model of a comb-like chain with $N_g = 5$ and $\sigma_s = 0.2$. (b) Simulation snapshots of conformations of comb-like chains with $N_g = 5$ and $\sigma_s = 0.2$, where k is 0.0, 0.5, and 2.0, respectively.

$$U_{\mathrm{WCA}}(r) = \begin{cases} 4\epsilon[(\sigma/r)^{12} - (\sigma/r)^6] + \epsilon, & r \le 2^{1/6}\sigma \\ 0, & r > 2^{1/6}\sigma \end{cases} \quad (4)$$

where r is the bead−bead distance and ϵ and σ represent the energy and length parameters, respectively. Adjacent beads in the backbone or side chains, including the grafting point between the beads of side chains and the backbone, are both connected by the finitely extension nonlinear elastic (FENE) potential,[45] i.e.

$$U_{\mathrm{FENE}}(r) = -0.5\kappa R_0^2 \ln[1 - (r/R_0)^2] \quad (5)$$

where κ is the spring constant and R_0 represents the maximum separation distance for r. The backbone rigidity is introduced by adding an angle-dependent bending energy between successive bonds,[46,47] i.e.

$$U_{\mathrm{bend}}(\theta) = k(1 - \cos\theta) \quad (6)$$

where θ is the complementary angle between subsequent bond vectors and k denotes the strength of the bending energy.

We use the BD simulations to calculate the motion of the bead i,[48] i.e.

$$\dot{\mathbf{r}}_i(t) = -\frac{1}{\xi}\nabla U_i + \frac{1}{\xi}\mathbf{f}_i(t) \quad (7)$$

Here, U_i is the sum of all WCA, FENE, and bending potentials discussed above, and ξ denotes the friction coefficient of beads in a solvent with viscosity η, based on the Stokes−Einstein relation, which can be calculated as $\xi = 6\pi\eta a$. $\mathbf{f}_i(t)$ represents a random force related to ξ by the fluctuation dissipation theorem $\langle \mathbf{f}_i(t)\mathbf{f}_j(t')\rangle = 2\xi k_B T\delta_{ij}\delta(t - t')\mathbf{I}$, where $\mathbf{I}$ is the unit tensor. The equations are integrated with an Euler integrator, and the intramolecular hydrodynamic interactions are not taken into account, which allows us to compute longer time steps with less computational effort. In this work, we only focus on the conformation of comb-like chains, ignoring the dynamic properties such as diffusion; therefore, this choice is reasonable and economical.

https://doi.org/10.1021/acsomega.2c08018
ACS Omega 2023, 8, 11177−11183

We simulate the conformation of a comb-like chain in a cubic box with dimensions of (D, D, D), where the periodic boundary conditions are imposed along all directions. In this work, σ, m, and ϵ are taken to be the units of length, mass, and energy, respectively, and the unit of time is $\tau = (m\sigma^2/\epsilon)^{1/2}$. We set the FENE parameters as $\kappa = 30$ and $R_0 = 1.5$, which can prevent chains crossing.[49] We fixed the temperature as $k_BT = 1.0$, the time step as $\Delta t = 10^{-4}$, and the friction coefficient as $\xi = 0.5$, respectively. In addition, the simulation box is fixed as $D = 150$, and the length of the backbone is fixed as $N_b = 120$. We assume that the side chains are uniformly grafted onto the backbone with different grafting densities, which are in the range $0 \le \sigma_s \le 1$. In each case, 100 samples were averaged with $5 \times 1 \times 10^8$ simulation steps. We tune k to investigate the conformation of comb-like chains, partly shown in Figure 1b, where a comb-like chain that is more and more extended with the increase of k is observed.

In order to distinguish the backbone rigidity, we specify that the backbone with $k > 0$ is a semiflexible chain, and the backbone with $k = 0$ is a flexible chain. As shown in Figure 2a, the ratio of the radius of gyration of the semiflexible backbone and flexible backbone ($R_{g,b}/R_{g0}$) continues to increase with the increase of k, which indicates that the backbone is significantly stretched. In addition, we calculate the persistence length of the backbone by the projection of the end-to-end distance vector ($\mathbf{R}_e$) on the ith bond vector ($\mathbf{r}_{i,i+1}$) of the backbone, i.e., $l_p^i = \langle \mathbf{r}_{i,i+1}/|\mathbf{r}_{i,i+1}| \cdot \mathbf{R}_e \rangle$.[35,50] Due to the greater freedom of the two ends of the backbone, l_p^i is the smallest at the ends of the backbone and develops a well-defined plateau in the middle, whose average value is defined as the effective persistence length (l_p). As shown in Figure 2b, the ratio of the persistence length of the semiflexible backbone and flexible backbone ($l_{p,b}/l_{p0}$) increases with the increase of k, and when $k = 4$, the persistence length of the semiflexible backbone is as much as five times that of the flexible backbone, which demonstrates that we can change the backbone rigidity by adjusting the value of k. With these foundations, we can examine the constraint of the backbone rigidity on the stiffening of backbone caused by side chains and then clarify its effect on the conformation of comb-like chains.

3. RESULTS AND DISCUSSION

We first calculate the ratio of the radius of gyration of comb-like chains and the semiflexible backbone ($R_g/R_{g,b}$) as a function of σ_s in Figure 3, which indicates that $R_g/R_{g,b}$ increases gradually with the increase of σ_s for different k. In Figure 3a, we assume $\beta = 0$ in eq 3, i.e., ignoring the graft−graft excluded-

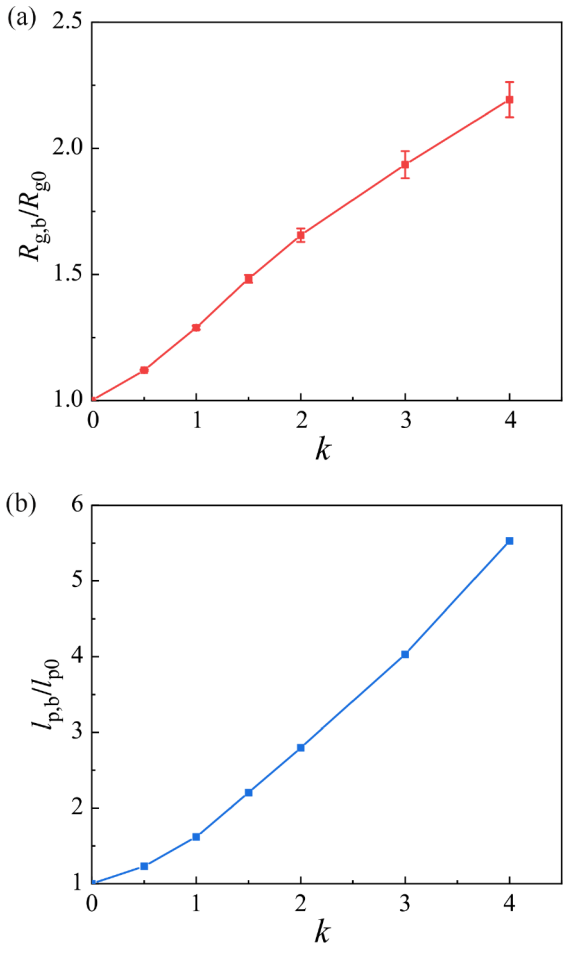

Figure 2. (a) Ratio of the radius of gyration of semiflexible backbone and flexible backbone ($R_{g,b}/R_{g0}$) as a function of the strength of bending energy (k). (b) Ratio of the persistence length of semiflexible backbone and flexible backbone ($l_{p,b}/l_{p0}$) as a function of the strength of bending energy (k).

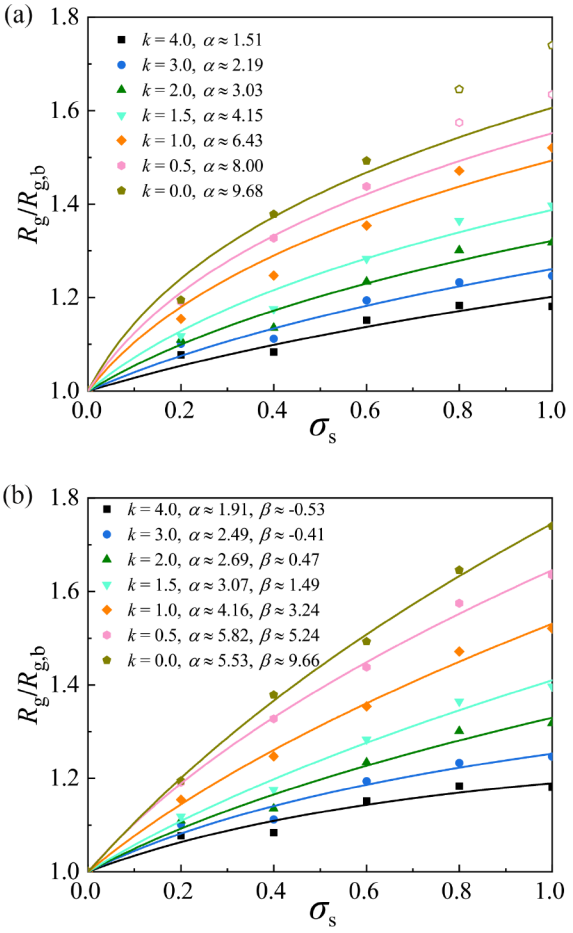

Figure 3. Ratio of the radius of gyration of comb-like chains and the semiflexible backbone ($R_g/R_{g,b}$) as a function of the graft density (σ_s) with different k, where the data are fitted by $R_g/R_{g,b} = (1 + \alpha\sigma_s)^{1/5}$ (a) and $R_g/R_{g,b} = (1 + \alpha\sigma_s + \beta\sigma_s^2)^{1/5}$ (b) in eq 3, respectively. The length of the side chains is fixed as $N_g = 5$. All hollow symbols refer specifically to the points that offset the fitting curves.

https://doi.org/10.1021/acsomega.2c08018
ACS Omega 2023, 8, 11177−11183

Table 1. Summary of Values of α and β Obtained by Fitting eq 3

	α				β			
k	$N_g = 1$	$N_g = 3$	$N_g = 5$	$N_g = 7$	$N_g = 1$	$N_g = 3$	$N_g = 5$	$N_g = 7$
0	0.82	2.91	5.53	6.67	1.08	3.62	9.66	18.67
0.5	0.70	2.61	5.82	6.86	0.68	1.64	5.24	12.71
1	0.28	1.74	4.16	5.54	0.63	0.77	3.24	7.53
1.5	−0.31	0.59	3.07	3.92	0.85	0.79	1.49	4.08
2	−0.48	0.19	2.69	3.73	0.89	0.73	0.47	1.71
3	−0.55	−0.11	2.49	3.32	0.85	0.64	−0.41	−0.12
4	−0.67	−0.29	1.91	2.53	0.82	0.58	−0.53	−0.57

volume interaction, and find that most of the data points can fall on the fitting curves. The results show that α gradually decreases as the increase in k (from 9.68 to 1.51), suggesting that the enhancement of backbone rigidity significantly weakens the relative strength of the excluded-volume interactions from backbone monomer−graft to backbone monomer−monomer. Only when $k = 0$ or $k = 0.5$ and σ_s is close to 1 do a few data points obviously deviate from the fitting curves. For $k = 0$ (the flexible backbone), when σ_s approaches 1, there are data points that do not conform to the assumption of $\beta = 0$. As we discussed in the previous work, under these conditions, the influence of the graft−graft excluded-volume interaction on conformations begins to become significant.[35] Importantly, we find that for $k = 0.5$ (the semiflexible backbone, $l_{p,b}/l_{p0} \approx 1.2$ in Figure 2b), similar to the results of $k = 0$, abnormal data points appear when σ_s tends to 1, which suggests that the increase of backbone rigidity is not enough to shield the effect of excluded-volume of side chains. But for most semiflexible backbones ($l_{p,b}/l_{p0} > 1.5$ in Figure 2b), the assumption of $\beta = 0$ is reasonable, which indicates that the graft−graft excluded-volume interaction can be ignored in the whole graft density range. Our results show that the change of backbone rigidity, especially the transition from flexible to semiflexible, has a significant impact on the relative strength of the excluded-volume interactions from graft−graft to backbone monomer−monomer.

We then examine the case when $\beta \neq 0$ in Figure 3b. The results show that all data points fall on the fitting curves, and α and β decrease simultaneously with the increase of k, indicating that the relative influence of backbone monomer−graft and graft−graft excluded-volume interactions is gradually weakened. In addition, β is greater than α on the rate of reduction, and when $k = 3$ or 4, the value of β is negative. In fact, when $k = 2$ ($l_{p,b}/l_{p0} \approx 3$ in Figure 2b), the value of β tends to zero, which means that the graft−graft excluded-volume interaction has little effect on the conformation of comb-like chains. From Figure 3a,b, we can conclude that, for the conformation of comb-like chains, the influence of excluded-volume interactions from the backbone monomer−graft always exists, and with the increase of backbone rigidity, its relative strength to the backbone monomer−monomer gradually weakens. However, the influence of graft−graft excluded-volume interaction appears and becomes important only when the backbone rigidity is relatively weak.

Finally, we summarize the values of α and β obtained by fitting different lengths of side chains in Table 1. We find that, for $N_g = 1$, the values of α and β are almost all less than 1, which means that when the length of side chains is a Kuhn length, the strength of the excluded-volume interactions from backbone monomer−graft and graft−graft is always lower than that of the backbone monomer−monomer. For other longer side chains, with the increase in k, the values of α and β both show a decreasing trend. The difference is that the value of β decreases faster, which indicates that the graft−graft-excluded volume interaction is more sensitive to the backbone rigidity. Based on existing data, we find that the growth of N_g can lead to the increase of α and β; that is, the relative strength of the excluded-volume interactions from backbone monomer−graft and graft−graft to backbone monomer−monomer increases gradually, but the increase of k can reduce the values of α and β, that is, it gradually shields the effect of steric repulsions caused by side chains. Our results demonstrate that the stiffening of the backbone can control the effect of excluded-volume interactions from the backbone monomer−graft and graft−graft, and it is meaningless to compare the impact of side chains without defining the backbone rigidity.

As shown in Figure 4, we explore the influence of the existence of side chains on the persistence length of the

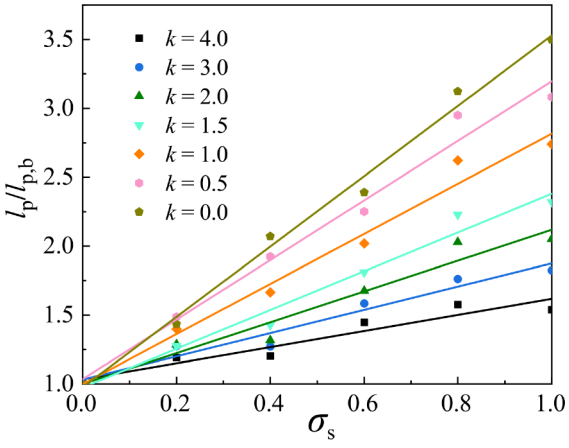

Figure 4. Ratio of the persistence length of the semiflexible backbone with grafting side chains and the semiflexible backbone ($l_p/l_{p,b}$) as a function of the grafting density (σ_s) with different k.

semiflexible backbone with grafting side chains. When we keep increasing σ_s, the ratio of the persistence length of semiflexible backbone with grafting side chains and the semiflexible backbone ($l_p/l_{p,b}$) increase almost linearly. Our results show that the steric repulsions caused by side chains increase the persistence length of the semiflexible backbone, but the influence gradually weakens with the increase of backbone rigidity. For example, for $k = 4$, when σ_s is changed from 0 to 1, the persistence length of the backbone increases by about 1.5 times, while for $k = 0.5$ it increases by about 3 times. In this work, we fix the length of the backbone as $N_b = 120$, whose persistence length is $l_{p0} \approx 4$, indicating $N_b/l_{p0} \approx 30$. But when $k = 4$, the persistence length of semiflexible backbone is $l_{p,b} \approx 23$,

https://doi.org/10.1021/acsomega.2c08018
ACS Omega 2023, 8, 11177−11183

indicating $N_b/l_{p,b} \approx 5$, which suggests that the backbone is relatively rigid. Within this stiffening range, our results demonstrate that the existence of side chains not only increases the persistence length of the backbone but also increases the size of comb-like chains. This trend slows with the increase in backbone rigidity.

In essence, increasing the grafting density or the length of side chains will increase the probability of contact between or within side chains, resulting in stronger steric repulsions, thereby changing the persistence length of the backbone and the conformation of the entire comb-like chain. Therefore, it is an effective way to describe the comb-like chains by the stretching factor ($\sigma_s N_g$). In Figure 5, we use the stretching factor to describe the size of comb-like chains and the persistence length of backbone. The results show that the radius of gyration of the comb-like chains and the persistence length of the backbone are exponentially related to the stretching factor, but the stiffness of the backbone is different, showing different exponential changes. For the radius of gyration of the comb-like chains, with the increase of k, its power exponent changes from less than 1 to more than 1, where the quasi linear relationship is that k is about 1.5 or 2.0. At this time, the persistence length of the semiflexible backbone is about 2.5 times that of the flexible backbone (Figure 2b). Differently, the persistence length of the semiflexible backbone with the grafted side chains changes from a quasi linear relationship to a power exponent greater than 1. Our results show that we can deduce the rigidity of the backbone by the power exponent between the size of comb-like chains and the stretching factor.

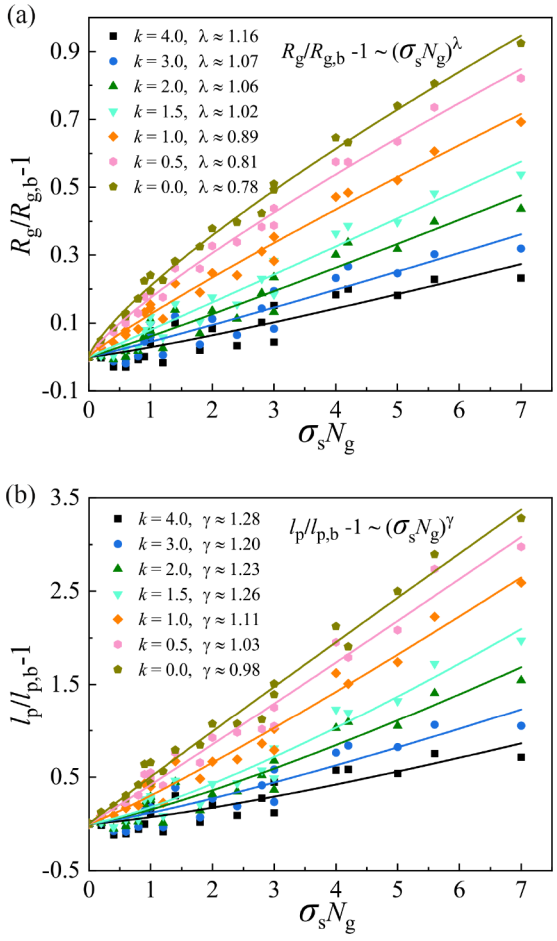

Figure 5. (a) Ratio of the radius of gyration of comb-like chains and the semiflexible backbone ($R_g/R_{g,b} - 1$) as a function of the stretching factor ($\sigma_s N_g$) with different k, where the data are fitted by $R_g/R_{g,b} - 1 \sim (\sigma_s N_g)^{\lambda}$. (b) Ratio of the persistence length of semiflexible backbone with grafting side chains and the semiflexible backbone ($l_p/l_{p,b} - 1$) as a function of the stretching factor ($\sigma_s N_g$) with different k, where the data are fitted by $l_p/l_{p,b} - 1 \sim (\sigma_s N_g)^{\gamma}$.

4. CONCLUSIONS

In summary, the current study clearly demonstrates that the backbone rigidity can control the effect of side chains on the conformation of comb-like chains; that is, the relative strength of the excluded-volume interactions from backbone monomer-graft and graft−graft to backbone monomer−monomer gradually weakens with the increase of backbone rigidity. Only when the rigidity of the backbone tends to the flexible and the grafting density is high is the effect of the excluded volume of graft−graft on the conformation of comb-like chains significant enough, and other cases can be ignored. Our results show that the radius of gyration of comb-like chains and the persistence length of the backbone are exponentially related to the stretching factor, where the power exponent exhibits an increase with the increase of the strength of bending energy.

In this work, we mainly focus on the semiflexible backbone, where the maximum ratio of the length of backbone to the persistence length is about 5. Obviously, when we continue to increase the stiffness of the backbone, especially for rigid chains, the steric repulsions caused by side chains will not be able to continue to increase the persistence length of the backbone. Therefore, the above will no longer apply to this special case. On the other hand, for short graft chains, it seems that the effect of their own stiffness should also be considered. However, since the graft chain is usually much shorter than the backbone, we speculate that their effect may be limited, especially in the case of high graft density, such as a bottle-brush chain. In conclusion, our work explains the effect of backbone rigidity on the conformation of comb-like chains and uncovers the contribution of excluded-volume interactions from side chains with different backbone rigidities, which provides a new insight for characterizing comb-like chains.

AUTHOR INFORMATION

Corresponding Author

Mingming Ding − *School of Chemical Engineering and Light Industry, Guangdong University of Technology, Guangzhou 510006, P.R. China; Xinjiang Laboratory of Phase Transitions and Microstructures in Condensed Matter Physics, College of Physical Science and Technology, Yili Normal University, Yining 835000, P.R. China;* orcid.org/0000-0002-9877-7699; Email: mmding@gdut.edu.cn

Authors

Xinghong Mai − *Xinjiang Laboratory of Phase Transitions and Microstructures in Condensed Matter Physics, College of Physical Science and Technology, Yili Normal University, Yining 835000, P.R. China*

Peng Hao − *Xinjiang Laboratory of Phase Transitions and Microstructures in Condensed Matter Physics, College of Physical Science and Technology, Yili Normal University, Yining 835000, P.R. China*

https://doi.org/10.1021/acsomega.2c08018
ACS Omega 2023, 8, 11177−11183

Danfeng Liu − *Xinjiang Laboratory of Phase Transitions and Microstructures in Condensed Matter Physics, College of Physical Science and Technology, Yili Normal University, Yining 835000, P.R. China*

Complete contact information is available at: https://pubs.acs.org/10.1021/acsomega.2c08018

Author Contributions

#X. Mai and P. Hao contributed equally to this work.

Notes

The authors declare no competing financial interest.

■ ACKNOWLEDGMENTS

This work is funded by the Scientific Research Project of Yili Normal University (2022YSYB012).

■ REFERENCES

(1) Pan, T.; Dutta, S.; Kamble, Y.; Patel, B. B.; Wade, M. A.; Rogers, S. A.; Diao, Y.; Guironnet, D.; Sing, C. E. Materials Design of Highly Branched Bottlebrush Polymers at the Intersection of Modeling, Synthesis, Processing, and Characterization. *Chem. Mater.* **2022**, *34*, 1990−2024.

(2) Li, Z.; Tang, M.; Liang, S.; Zhang, M.; Biesold, G. M.; He, Y.; Hao, S.-M.; Choi, W.; Liu, Y.; Peng, J.; Lin, Z. Bottlebrush polymers: From controlled synthesis, self-assembly, properties to applications. *Prog. Polym. Sci.* **2021**, *116*, 101387.

(3) Mohammadi, E.; Joshi, S. Y.; Deshmukh, S. A. A review of computational studies of bottlebrush polymers. *Comput. Mater. Sci.* **2021**, *199*, 110720.

(4) Zhao, B. Shape-Changing Bottlebrush Polymers. *J. Phys. Chem. B* **2021**, *125*, 6373−6389.

(5) Xie, G.; Martinez, M. R.; Olszewski, M.; Sheiko, S. S.; Matyjaszewski, K. Molecular Bottlebrushes as Novel Materials. *Biomacromolecules* **2019**, *20*, 27−54.

(6) Verduzco, R.; Li, X.; Pesek, S. L.; Stein, G. E. Structure, function, self-assembly, and applications of bottlebrush copolymers. *Chem. Soc. Rev.* **2015**, *44*, 2405−2420.

(7) Sheiko, S. S.; Sumerlin, B. S.; Matyjaszewski, K. Cylindrical molecular brushes: Synthesis, characterization, and properties. *Prog. Polym. Sci.* **2008**, *33*, 759−785.

(8) Terao, K.; Nakamura, Y.; Norisuye, T. Solution properties of polymacromonomers consisting of polystyrene. 2. Chain dimensions and stiffness in cyclohexane and toluene. *Macromolecules* **1999**, *32*, 711−716.

(9) Hokajo, T.; Terao, K.; Nakamura, Y.; Norisuye, T. Solution properties of polymacromonomers consisting of polystyrene - V. Effect of side chain length on chain stiffness. *Polym. J.* **2001**, *33*, 481−485.

(10) Abbasi, M.; Faust, L.; Wilhelm, M. Comb and Bottlebrush Polymers with Superior Rheological and Mechanical Properties. *Adv. Mater.* **2019**, *31*, 1806484.

(11) Johnson, J. A.; Lu, Y. Y.; Burts, A. O.; Lim, Y.-H.; Finn, M. G.; Koberstein, J. T.; Turro, N. J.; Tirrell, D. A.; Grubbs, R. H. Core-Clickable PEG-Branch-Azide Bivalent-Bottle-Brush Polymers by ROMP: Grafting-Through and Clicking-To. *J. Am. Chem. Soc.* **2011**, *133*, 559−566.

(12) Watanabe, M.; Mizukami, K. Well-Ordered Wrinkling Patterns on Chemically Oxidized Poly(dimethylsiloxane) Surfaces. *Macromolecules* **2012**, *45*, 7128−7134.

(13) Seong, H.-G.; Chen, Z.; Emrick, T.; Russell, T. P. Reconfiguration and Reorganization of Bottlebrush Polymer Surfactants. *Angew. Chem., Int. Ed.* **2022**, *61*, e202200530.

(14) Pesek, S. L.; Lin, Y.-H.; Mah, H. Z.; Kasper, W.; Chen, B.; Rohde, B. J.; Robertson, M. L.; Stein, G. E.; Verduzco, R. Synthesis of bottlebrush copolymers based on poly(dimethylsiloxane) for surface active additives. *Polymer* **2016**, *98*, 495−504.

(15) Unsal, H.; Onbulak, S.; Calik, F.; Er-Rafik, M.; Schmutz, M.; Sanyal, A.; Rzayev, J. Interplay between Molecular Packing, Drug Loading, and Core Cross-Linking in Bottlebrush Copolymer Micelles. *Macromolecules* **2017**, *50*, 1342−1352.

(16) Fredrickson, G. H. Surfactant-induced lyotropic behavior of flexible polymer solutions. *Macromolecules* **1993**, *26*, 2825−2831.

(17) Rouault, Y.; Borisov, O. V. Comb-Branched Polymers: Monte Carlo Simulation and Scaling. *Macromolecules* **1996**, *29*, 2605−2611.

(18) Feuz, L.; Leermakers, F. A. M.; Textor, M.; Borisov, O. Bending Rigidity and Induced Persistence Length of Molecular Bottle Brushes: A Self-Consistent-Field Theory. *Macromolecules* **2005**, *38*, 8891−8901.

(19) Zhang, B.; Gröhn, F.; Pedersen, J. S.; Fischer, K.; Schmidt, M. Conformation of Cylindrical Brushes in Solution: Effect of Side Chain Length. *Macromolecules* **2006**, *39*, 8440−8450.

(20) Dutta, S.; Pan, T.; Sing, C. E. Bridging Simulation Length Scales of Bottlebrush Polymers Using a Wormlike Cylinder Model. *Macromolecules* **2019**, *52*, 4858−4874.

(21) Morozova, S.; Lodge, T. P. Conformation of Methylcellulose as a Function of Poly(ethylene glycol) Graft Density. *ACS Macro Lett.* **2017**, *6*, 1274−1279.

(22) Nakamura, Y.; Norisuye, T. Backbone stiffness of comb-branched polymers. *Polym. J.* **2001**, *33*, 874−878.

(23) Morozova, S.; Schmidt, P. W.; Bates, F. S.; Lodge, T. P. Effect of Poly(ethylene glycol) Grafting Density on Methylcellulose Fibril Formation. *Macromolecules* **2018**, *51*, 9413−9421.

(24) Pan, X.; Ishaq, M. W.; Umair, A.; Ali, M. W.; Li, L. Evolution of Single Chain Conformation for Model Comb-Like Chains with Grafting Density Ranging from 0 to 100% in Dilute Solution. *ACS Macro Lett.* **2019**, *8*, 1535−1540.

(25) Pan, X.; Ding, M.; Li, L. Experimental Validation on Average Conformation of a Comblike Polystyrene Library in Dilute Solutions: Universal Scaling Laws and Abnormal SEC Elution Behavior. *Macromolecules* **2021**, *54*, 11019−11031.

(26) Pan, X.; Ishaq, M. W.; Ali, M. W.; Yang, J.; Li, L.; Chen, Y. Unraveling the conformational properties of comb-like Poly-(propargyl acrylate)-graft-poly(2-ethyl-2-oxazoline) chains in dilute solutions. *Polymer* **2021**, *233*, 124224.

(27) Yethiraj, A. A Monte Carlo simulation study of branched polymers. *J. Chem. Phys.* **2006**, *125*, 204901.

(28) Theodorakis, P. E.; Hsu, H.-P.; Paul, W.; Binder, K. Computer simulation of bottle-brush polymers with flexible backbone: Good solvent versus theta solvent conditions. *J. Chem. Phys.* **2011**, *135*, 164903.

(29) Chatterjee, D.; Vilgis, T. A. Scaling Laws of Bottle-Brush Polymers in Dilute Solutions. *Macromol. Theory Simul.* **2016**, *25*, 518−523.

(30) Dutta, S.; Wade, M. A.; Walsh, D. J.; Guironnet, D.; Rogers, S. A.; Sing, C. E. Dilute solution structure of bottlebrush polymers. *Soft Matter* **2019**, *15*, 2928−2941.

(31) Bejagam, K. K.; Singh, S. K.; Ahn, R.; Deshmukh, S. A. Unraveling the Conformations of Backbone and Side Chains in Thermosensitive Bottlebrush Polymers. *Macromolecules* **2019**, *52*, 9398−9408.

(32) Mai, D. J.; Marciel, A. B.; Sing, C. E.; Schroeder, C. M. Topology-Controlled Relaxation Dynamics of Single Branched Polymers. *ACS Macro Lett.* **2015**, *4*, 446−452.

(33) Horkay, F.; Chremos, A.; Douglas, J. F.; Jones, R. L.; Lou, J.; Xia, Y. Systematic investigation of synthetic polyelectrolyte bottle-brush solutions by neutron and dynamic light scattering, osmometry, and molecular dynamics simulation. *J. Chem. Phys.* **2020**, *152*, 194904.

(34) Horkay, F.; Chremos, A.; Douglas, J. F.; Jones, R.; Lou, J.; Xia, Y. Comparative experimental and computational study of synthetic and natural bottlebrush polyelectrolyte solutions. *J. Chem. Phys.* **2021**, *155*, 074901.

(35) Tang, Z.; Pan, X.; Zhou, H.; Li, L.; Ding, M. Conformation of a Comb-like Chain Free in Solution and Confined in a Nanochannel: From Linear to Bottlebrush Structure. *Macromolecules* **2022**, *55*, 8668−8675.

(36) Rathgeber, S.; Pakula, T.; Wilk, A.; Matyjaszewski, K.; Beers, K. L. On the shape of bottle-brush macromolecules: Systematic variation of architectural parameters. *J. Chem. Phys.* **2005**, *122*, 124904.
(37) Hsu, H. P.; Paul, W.; Rathgeber, S.; Binder, K. Characteristic Length Scales and Radial Monomer Density Profiles of Molecular Bottle-Brushes: Simulation and Experiment. *Macromolecules* **2010**, *43*, 1592−1601.
(38) Hsu, H. P.; Paul, W.; Binder, K. Standard Definitions of Persistence Length Do Not Describe the Local "Intrinsic" Stiffness of Real Polymer Chains. *Macromolecules* **2010**, *43*, 3094−3102.
(39) Hsu, H. P.; Paul, W.; Binder, K. Understanding the Multiple Length Scales Describing the Structure of Bottle-brush Polymers by Monte Carlo Simulation Methods. *Macromol. Theory Simul.* **2011**, *20*, 510−525.
(40) Lyubimov, I.; Wessels, M. G.; Jayaraman, A. Molecular Dynamics Simulation and PRISM Theory Study of Assembly in Solutions of Amphiphilic Bottlebrush Block Copolymers. *Macromolecules* **2018**, *51*, 7586−7599.
(41) Wessels, M. G.; Jayaraman, A. Molecular dynamics simulation study of linear, bottlebrush, and star-like amphiphilic block polymer assembly in solution. *Soft Matter* **2019**, *15*, 3987−3998.
(42) Mai, D. J.; Saadat, A.; Khomami, B.; Schroeder, C. M. Stretching Dynamics of Single Comb Polymers in Extensional Flow. *Macromolecules* **2018**, *51*, 1507−1517.
(43) Patel, S. F.; Young, C. D.; Sing, C. E.; Schroeder, C. M. Nonmonotonic dependence of comb polymer relaxation on branch density in semidilute solutions of linear polymers. *Phys. Rev. Fluids* **2020**, *5*, 121301.
(44) Weeks, J. D.; Chandler, D.; Andersen, H. C. Role of Repulsive Forces in Determining the Equilibrium Structure of Simple Liquids. *J. Chem. Phys.* **1971**, *54*, 5237−5247.
(45) Kremer, K.; Grest, G. S. Dynamics of entangled linear polymer melts: A molecular-dynamics simulation. *J. Chem. Phys.* **1990**, *92*, 5057−5086.
(46) Haakansson, C.; Elvingson, C. Semiflexible Chain Molecules with Nonuniform Curvature. 1. Structural Properties. *Macromolecules* **1994**, *27*, 3843−3849.
(47) Nikoubashman, A.; Milchev, A.; Binder, K. Dynamics of single semiflexible polymers in dilute solution. *J. Chem. Phys.* **2016**, *145*, 234903.
(48) Ermak, D. L.; McCammon, J. A. Brownian dynamics with hydrodynamic interactions. *J. Chem. Phys.* **1978**, *69*, 1352−1360.
(49) Kumar, S.; Larson, R. G. Brownian dynamics simulations of flexible polymers with spring−spring repulsions. *J. Chem. Phys.* **2001**, *114*, 6937−6941.
(50) Elli, S.; Ganazzoli, F.; Timoshenko, E. G.; Kuznetsov, Y. A.; Connolly, R. Size and persistence length of molecular bottle-brushes by Monte Carlo simulations. *J. Chem. Phys.* **2004**, *120*, 6257−6267.

https://doi.org/10.1021/acsomega.2c08018
ACS Omega 2023, 8, 11177−11183